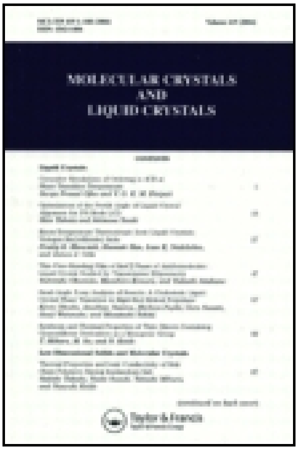

Molecular Crystals and Liquid Crystals
Publication details, including instructions for authors and subscription information:
http://www.tandfonline.com/loi/gmcl20

INTERFACIAL PROPERTIES OF POLYMER-LIQUID CRYSTAL

Akihiko Matsuyama[a]
[a] Department of Chemistry for Materials, Faculty of Engineering, Mie University, Tsu Mie 514-8507, Japan

To cite this article: Akihiko Matsuyama (2004): INTERFACIAL PROPERTIES OF POLYMER-LIQUID CRYSTAL, Molecular Crystals and Liquid Crystals, 413:1, 171-177

To link to this article: http://dx.doi.org/10.1080/15421400490437187

Mol. Cryst. Liq. Cryst., Vol. 413, pp. 171/[2307]–177/[2313], 2004
Copyright © Taylor & Francis Inc.
ISSN: 1542-1406 print/1563-5287 online
DOI: 10.1080/15421400490437187

INTERFACIAL PROPERTIES OF POLYMER-LIQUID CRYSTAL

Akihiko Matsuyama
Department of Chemistry for Materials, Faculty of Engineering,
Mie University, Tsu Mie 514-8507, Japan

We theoretically study interfacial properties between two coexisting phases in mixtures of a flexible polymer and a low molecular weight liquid crystal. By numerically solving Eular equations for concentration and orientation order parameters, we calculate order parameter profiles and interfacial tensions between coexisting nematic-isotopic and isotropic-isotropic phases at equilibrium.

Keywords: Eular equations; interfacial properties; interfacial tension; nematic-isotropic transition; polymer-liquid crystal mixtures

1. INTRODUCTION

Interfacial properties with concentration and orientation order parameters have been studied for a free surface of pure liquid crystals [1] and interfacial tension between coexisting isotropic and nematic phases of semiflexible polymers [2,3]. Some authors theoretically studied the interfacial tension of mixtures of a polymer and a liquid crystal based on the lattice Monte Carlo simulation [4] and the Helfand lattice theory [5]. Smith *et al.* measured the interfacial tension of a nematic liquid crystal (5CB) immersed in polydimethylsiloxane (PDMS) matrix and showed that the interfacial free energy is decreased as the temperature is increased [6].

In this paper we theoretically study interfacial properties between coexisting phases at equilibrium in mixtures of a flexible polymer and a low molecular weight liquid crystal [7–9]. By numerically solving Eular equations for concentration and orientation order parameters, we calculate interfacial tension and order parameter profiles at equilibrium as a function

---

Address correspondence to Akihiko Matsuyama, Department of Chemistry for Materials, Faculty of Engineering, Mie University, Tsu Mie 514-8507, Japan.

of temperature. We find strong temperature dependencies of the interfacial tension and non-monotonic behaviors of the order parameter profiles.

2. GENERAL TREATMENT OF AN INTERFACIAL TENSION

We consider a flat interface (x-y plane) of the area $\mathbf{\Omega}$ between coexisting nematic (or isotropic) and isotropic phases in a binary mixture and take the z-axis perpendicular to the plane interface. The following analysis is valid for any systems which have compositional (ϕ) and orientational (S) order parameters. Let ϕ_n be the equilibrium concentration (volume fraction) of the nematic phase with the orientational order parameter S_n and ϕ_0 be the volume fraction of the isotropic phase.

In the nonuniform system near an interface, spatial variations occur in the two order parameters. The total free energy (F) can be expressed in terms of a local bulk free energy density $f(\phi, S)$ and the gradients of the two order parameters:

$$F = \mathbf{\Omega} \int_{-\infty}^{\infty} dz \left[f(\phi, S) + K_\phi (\nabla \phi)^2 + K_0 (\nabla \phi)(\nabla S) + K_S (\nabla S)^2 \right], \qquad (1)$$

where $\nabla \equiv d/dz$ and we assume that coefficients K_ϕ, K_0, and K_S are constants for a simplicity. The specific interfacial free energy γ is defined by the difference per unit area of the interface between the autual free energy of the system and that of the isotropic bulk free energy:

$$\gamma = \int_{-\infty}^{\infty} dz \left[\Delta f(\phi, S) + K_\phi (\Delta \phi)^2 + K_0 (\nabla \phi)(\nabla S) + K_S (\nabla S)^2 \right], \qquad (2)$$

where $\Delta f(\phi, S)$ is defined by [10]

$$\Delta f(\phi, S) = f(\phi, S) - f(\phi_0, 0) - (\phi - \phi_0)(df/d\phi)_{\phi=\phi_0}. \qquad (3)$$

By substituting the integration of Eq. (2) into the Eular equation, we obtain the coupled differential equations whose solutions are the composition and orientation profiles corresponding to a stationary value:

$$2K_\phi \nabla^2 \phi + K_0 \nabla^2 S = (\partial \Delta f / \partial \phi), \qquad (4)$$

$$2K_S \nabla^2 S + K_0 \nabla^2 \phi = (\partial \Delta f / \partial S). \qquad (5)$$

To be physically acceptable, the solutions of Eqs. (4) and (5) have to satisfy the following boundary conditions:

$$d\phi/dz = 0, \quad dS/dz = 0, \qquad (6)$$

and

$$\Delta f(\phi,S) = 0, \tag{7}$$

at $z = \pm\infty$. We also define $\phi_0 = \phi(-\infty), \phi_n = \phi(\infty)$, and $S_n = S(\infty)$. Multiplying Eq. (4) by $(d\phi/dz)$ and Eq. (5) by (dS/dz), adding the resulting equations, and then integrating once with respect to z, we obtain the condition for a stationary solution:

$$\Delta f(\phi,S) = K_\phi(\nabla\phi)^2 + K_0(\nabla\phi)(\nabla S) + K_S(\nabla S)^2. \tag{8}$$

Using this expression to eliminate the gradient terms from Eq. (2), the interfacial tension is given by

$$\gamma = 2\int_{-\infty}^{\infty} \Delta f(\phi(z),S(z))dz. \tag{9}$$

3. APPLICATION OF POLYMER-LIQUID CRYSTAL MIXTURES

In this section we apply the above results to mixtures of a flexible polymer and a liquid crystal.

The dimensionless equilibrium free energy density $f(\phi,S)$ of polymer-liquid crystal mixtures is given by combining the Flory-Huggins theory for isotropic mixing of two components with the free energy for nematic ordering [9,11]:

$$\begin{aligned} f(\phi,S) = {} & \frac{1-\phi}{n_p}\ln(1-\phi) + \frac{\phi}{n_l}\ln\phi + \chi\phi(1-\phi) \\ & + \nu\phi^2\left[\frac{1}{2}\left(1-\frac{\eta}{3}\right)S^2 - \frac{\eta}{9}S^3 + \frac{\eta}{6}S^4\right] \end{aligned} \tag{10}$$

where ϕ is the volume fraction of the nematogens and S is the 'scalar' orientational order parameter of the nematogens, n_p is the number of segments on the polymer, n_l is axis ratio of the nematogen, and $\eta \equiv n_l\nu\phi$. The value $\chi(\equiv U_0/k_BT)$ is the Flory-Huggins interaction parameter related to isotropic interactions between unlike molecular species and $\nu(\equiv U_a/k_BT)$ parametrizes the orientation-dependent (Maier-Saupe) interactions between the nematogens [13,14]. We here introduce two typical phase diagrams on the temperature-concentration plane [9].

Figure 1(a) shows the phase diagram for $n_p = 10$, $n_l = 2$ and $\nu/\chi = 5$. The reduced temperature $\tau(\equiv T/T_{NI})$ is normalized by the NIT tempera-

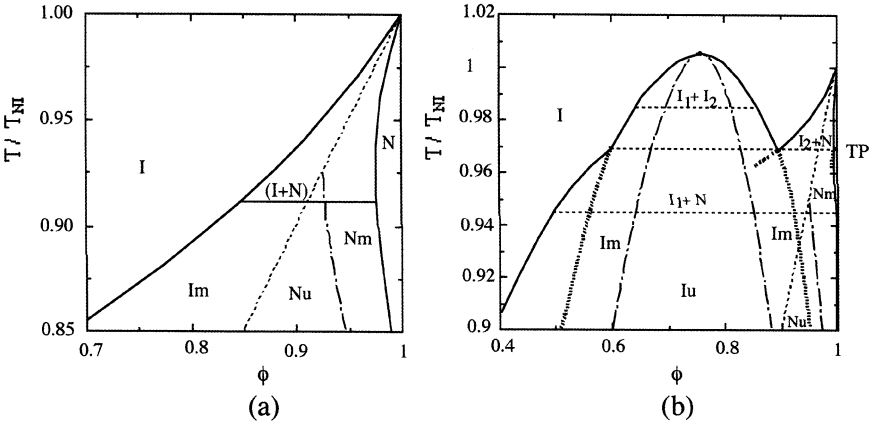

(a) (b)

FIGURE 1 (a) Phase diagram for $n_p = 10, n_l = 2$ and $\nu/\chi = 5$. (b) phase diagram with a triple point for $n_p = 20, n_l = 2$ and $\nu/\chi = 3.1$.

ture (T_{NI}) of the pure nematogen. The solid curve refers to the binodal and the dotted line shows the first-order NIT line. The dash-dotted line shows the spinodal. Below the T_{NI}, we have the two-phase coexistence between an isotropic and a nematic phase ($I + N$) for all temperature ranges. As decreasing temperature, the biphasic region have two different metastable regions: an isotropic metastable (Im) and a nematic metastable (Nm), and a nematic unstable (Nu) [9].

As increasing the number n_p of segments on the polymer, we have a phase diagram with a triple point. Figure 1(b) shows the phase diagram for $n_p = 20, n_l = 2$ and $\nu/\chi = 3.1$. When $\tau = 0.969$, we have a triple point (TP) where two isotropic liquid phases ($I_1 + I_2$) and a nematic phase (N) can simultaneously coexist. Below the TP temperature, we have the two-phase coexistence between an isotropic (I_1) and a nematic (N) phase. Hereafter $I_1(I_2)$ refers to the isotropic liquid phase of lower (higher) concentrations on the phase diagram. The closed circle shows a critical point for the ($I_1 + I_2$) phase separation.

In the following subsections, we show our numerical results for the interfacial properties between the coexisting phases on the phase diagrams. To calculate the interfacial tension between an isotropic and a nematic (or isotropic) phase, we first numerically solve the Euler equations (4) and (5) to obtain stationary solutions for the profiles of concentration and orientational order, corresponding to the lowest interfacial energy. We here set $K_\phi = 0.4$, $K_0 = -0.01$, and $K_S = 0.01$ for a typical example. When $K_0 < 0$, the director is parallel to the interface.

3.1. Isotropic-Nematic Interface

In this subsection we show the interfacial properties between the isotropic-nematic phases $(I+N)$ on the phase diagram of Figure 1(a). Figure 2 shows the interfacial profiles of $\phi(z)$ (solid line) and $S(z)$ (dotted line) at $\tau = 0.998$. When $\tau = 0.998$, the value of $S(z)$ is changed monotonously from zero to S_n and the concentration $\phi(z)$ exhibits a non-monotonous behavior. The concentration profile has a small minimum in the isotropic phase (z < 0) of the interfacial region. This indicates that the nematic phase behaves as a wall (depletion zone) excluding nematogens in the isotropic phase of the interfacial region. When the difference of the concentrations between the two coexisting phases is very small, the flexible polymers tend to gather in the two coexisting phases is very small, the flexible polymers tend to gather in the interfacial region. As decreasing temperature, the phase boundary becomes broad and the minimum in the concentration profile disappears. Figure 3 shows the interfacial tension (γ) between the $(I+N)$ phases plotted against the reduced temperature (τ). The reduced interfacial tension γ/γ_{NI} is normalized by the interfacial tension (γ_{NI}) for the isotropic-nematic interface of the pure nematogen ($\phi = 1$) at $\tau = 1$. As decreasing temperature, the interfacial tension is rapidly increased. Similar behaviors have been calculated by a Monte Carlo simulation [4]. We find the interfacial tansion is proportional to

$$\gamma/\gamma_{NI} \propto (1 - T/T_{NI})^{2.5}, \tag{11}$$

at lower temperature as shown on the inset of Figure 3. Such strong temperature dependence comes from not only concentration gradient but also orientation gradient.

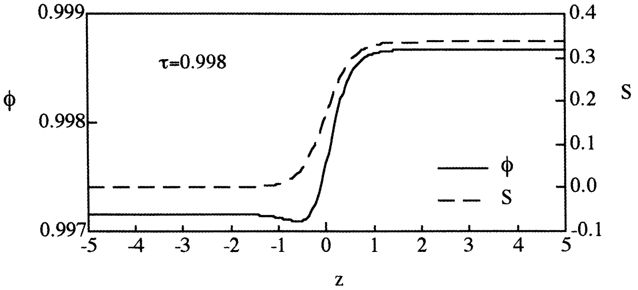

FIGURE 2 Interfacial profiles of $\phi(z)$ (solid line) and *S(z)* (dotted line) at $\tau = 0.998$ on Figure 1(a).

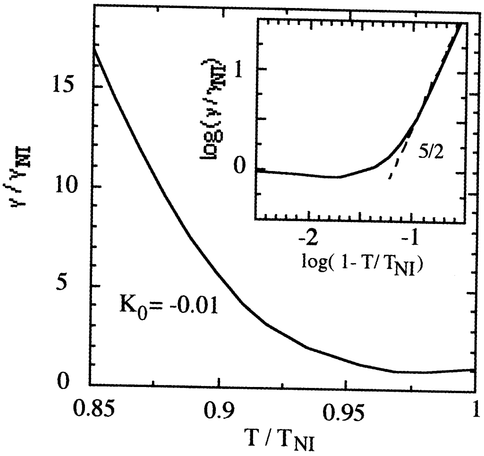

FIGURE 3 Interfacial tension (γ) between the I and N phases plotted against the reduced temperature (τ).

3.2. Isotropic-Nematic Interface Near a Triple Point

In this subsection we show the interfacial properties between coexisting isotropic and nematic phases ($I_1 + N$) near the TP on the phase diagram of Figure 1(b).

Figure 4 shows the reduced interfacial tension (γ/γ_{NI}) of the $I_1 + N$ and $I_2 + N$ interfaces plotted against the reduced temperature (τ). As decreas-

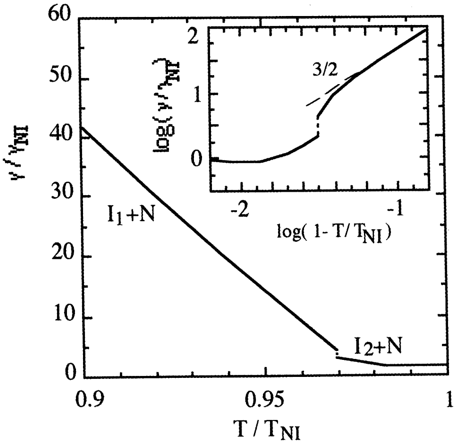

FIGURE 4 Reduced interfacial tension (γ/γ_{NI}) of the $I_1 + N$ and $I_2 + N$ interfaces on Figure 1(b) plotted against the reduced temperature (τ).

ing temperature the interfacial tension is increased and jumps at the TP temperature. At lower temperatures of the TP, the interfacial tension is proportional to

$$\gamma/\gamma_{NI} \propto (1 - T/T_{NI})^{1.5}, \tag{12}$$

as shown on the inset of Figure 4. The power law 1.5 is the same value as the temperature dependence of the interfacial tension for the isotropic-isotropic interface [15,16]. As shown in Figure 1(b), the isotropic unstable region (Iu) appears in the phase diagram and we have a broad biphasic region. As decreasing temperature the contribution from the concentration gradients becomes dominant in the interfacial free energy and then we can expect the same power law 1.5 as that of the isotropic-isotropic interface.

In conclusion, we find that the interfacial tension between coexisting nematic and isotropic phases is increased with decreasing temperature and is proportional to $\gamma/\gamma_{NI} \propto (1 - T/T_{NI})^n$ at lower temperatures. The power law n is affected by the existence of the TP. For the phase diagram in the presence of the TP, the power law n approaches to 1.5 as decreasing temperature below the TP. On the other hand, for the phase diagram in the absence of the TP, we have the power law 2.5 at lower temperatures. Such strong power law has not been experimentally observed yet.

REFERENCES

[1] de Gennes, P. G. (1971). *Mol. Cryst. Liq. Cryst.*, *12*, 193.
[2] Koch, D. L. & Harlen, O. G. (1999). *Macromolecules*, *32*, 219.
[3] Fukuda, J. (1999). *Eur. Phys. J. B*, *7*, 573.
[4] Zhu, J., Ding, J., Lu, J., & Yang, Y. (1998). *Polymer*, *39*, 6455.
[5] Chen, Y., Li, J., Zhang, H., & Yang, Y. (1995). *Mol. Cryst. Liq. Cryst.*, *258*, 37.
[6] Smith, G. W., Vaz, N. A., & Vansteenkiste, T. H. (1989). *Mol. Cryst. Liq. Cryst.*, *174*, 49.
[7] Yang, Y., Lu, J., Zhang, H., & Yu, T. (1994). *Polym. J.*, *26*, 880.
[8] Shen, C. & Kyu, T. (1995). *J. Chem. Phys.*, *102*, 556.
[9] Matsuyama, A. & Kato, T. (1996). *J. Chem. Phys.*, *105*, 1654; (1998). *108*, 2067; (1999). *Phys. Rev. E*, *59*, 763.
[10] Cahn, J. W. & Hillard, J. E. (1957). *J. Chem. Phys.*, *28*, 258. (1959). *31*, 688.
[11] Doi, M. & Edwards, S. F. (1986). *Theory of Polymer Dynamics*, Academic: New York.
[12] Flory, P. J. (1953). *Principles of Polymer Chemistry*, Cornell University: Ithaca.
[13] Maier, W., Saupe, A., & Naturforsch, Z. (1959). A *14a*, 882.
[14] de Gennes, P. G. & Prost, J. (1993). *The Physics of Liquid Crystals*, 2nd ed., Oxford. Sci.: London.
[15] Carton, J. P. & Leibler, L. (1990). *J. Phys. France*, *51*, 1683.
[16] Shinozaki, K., Tan, T. V., Saito, Y., & Nose, T. (1982). *Polymer*, *23*, 728.